

# Photochemical & Photobiological Sciences

Accepted Manuscript



This is an *Accepted Manuscript*, which has been through the Royal Society of Chemistry peer review process and has been accepted for publication.

*Accepted Manuscripts* are published online shortly after acceptance, before technical editing, formatting and proof reading. Using this free service, authors can make their results available to the community, in citable form, before we publish the edited article. We will replace this *Accepted Manuscript* with the edited and formatted *Advance Article* as soon as it is available.

You can find more information about *Accepted Manuscripts* in the [Information for Authors](#).

Please note that technical editing may introduce minor changes to the text and/or graphics, which may alter content. The journal's standard [Terms & Conditions](#) and the [Ethical guidelines](#) still apply. In no event shall the Royal Society of Chemistry be held responsible for any errors or omissions in this *Accepted Manuscript* or any consequences arising from the use of any information it contains.

1 Submitted to Photochemical & Photobiological Sciences

2 To the “Communication” section

3

4 **First detection of the presence of naturally occurring grapevine downy mildew in the**  
5 **field by a fluorescence-based method†**

6

7 Gwendal Latouche<sup>1</sup>, Christian Debord<sup>2</sup>, Marc Raynal<sup>2</sup>, Charlotte Milhade<sup>3</sup> & Zoran G.

8 Cerovic<sup>1\*</sup>

9

10 <sup>1</sup>Univ Paris-Sud, Laboratoire Ecologie Systématique et Evolution, UMR8079, Bât 362,  
11 Orsay, F-91405; CNRS, Orsay, F-91405; AgroParisTech, Paris, F-75231, France

12 <sup>2</sup>Institut Français de la Vigne et du Vin, Vinopole, 39 rue Montaigne, Blanquefort, F-33290,  
13 France

14 <sup>3</sup>FORCE-A. Univ. Paris-Sud, Bât. 503, Orsay, F-91405, France

15 \*Corresponding author

16 Email: [zoran.cerovic@u-psud.fr](mailto:zoran.cerovic@u-psud.fr), Tel: +33169157224, Fax: +33169157353

17

18

19 Early detection of fungal pathogen presence in the field would help to better time or avoid  
20 some of the fungicide treatments used to prevent crop production losses. We recently  
21 introduced a new phytoalexin-based method for a non-invasive detection of crop diseases  
22 using their fluorescence. The causal agent of grapevine downy mildew, *Plasmopara viticola*,  
23 induces the synthesis of stilbenoid phytoalexins by the host, *Vitis vinifera*, early upon  
24 infection. These stilbenoids emit violet-blue fluorescence under UV light. A hand-held solid-  
25 state UV-LED-based field fluorimeter, named Multiplex 330, was used to measure stilbenoid  
26 phytoalexins in a vineyard. It allowed us to non-destructively detect and monitor the naturally  
27 occurring downy mildew infections on leaves in the field.

28

29 Footnote

30 †Electronic supplementary information (ESI) available: Fig. S1. Temperature and  
31 precipitation for the surveyed vineyard in 2014; Fig. S2. Violet-blue fluorescence signals  
32 during the period before the onset of downy mildew infection compared to the black rot  
33 disease incidence; Fig. S3. Example of the variability of the violet-blue fluorescence signals.

34 See DOI:

## 35 Introduction

36 Viticulture and winemaking are both important economic activities and cultural issues in  
37 Europe. To protect their grapevines, European wine growers use 70,000 tons of pesticides  
38 each year that cost almost two billion euros<sup>1</sup>. Most are fungicides, because fungal diseases can  
39 induce crop losses up to 70%<sup>2</sup>. This is the motivation behind the European directive  
40 128/2009/EC, whose aims is to implement a more sustainable approach to the use of plant  
41 protection products.

42 Fungicides aim to prevent two main diseases, powdery mildew and downy mildew, the  
43 latter being usually considered as the most damaging disease in viticulture. The downy  
44 mildew infectious agent is an oomycete named *Plasmopara viticola* (Berk. & M.A. Curtis)  
45 Berl. & de Toni<sup>2</sup>. After one to two weeks of being present in the leaf it produces visible  
46 symptoms known as oil spots. One of the reactions of plants to both downy and powdery  
47 mildew is the synthesis of a variety of stilbenoid compounds. A useful characteristic of  
48 grapevine phytoalexins is that they produce a UV-induced violet-blue fluorescence (VBF). *In*  
49 *vitro*, the excitation maximum is at 320 nm<sup>3,4</sup> and the fluorescence emission maximum at 380  
50 nm<sup>3,4</sup>. *In vivo*, they are slightly shifted to longer wavelengths, with the excitation maximum at  
51 330 nm<sup>3,5</sup> and the emission maximum at around 400 nm<sup>5</sup>.

52 This autofluorescent property of the stilbenoid phytoalexins, which are absent from  
53 healthy leaves<sup>5</sup>, was exploited to detect the presence of downy mildew in greenhouse-grown  
54 plants<sup>4,6</sup>, in outdoors-grown plants<sup>5,6</sup> and in the field<sup>7</sup>. Microscopic studies on live leaf pieces  
55 have shown that the fluorescence is mainly localised in epidermal cell walls close to the leaf  
56 surface<sup>3,4</sup>.

57 The development of a portable fluorescence sensor<sup>5</sup>, Multiplex 330 (FORCE-A, Orsay,  
58 France), hereafter Mx-330, allowed the application of this diagnostic method to leaves  
59 attached to the plant. In the greenhouse, infected leaves could be discriminated from control  
60 leaves from the first day post infection (DPI) on the abaxial side of leaves and the DPI 3 on  
61 the adaxial side<sup>5</sup>. In the field, infected leaves could be discriminated from control ones  
62 starting from DPI 6 on both sides<sup>7</sup>. This is encouraging because there is a higher probability  
63 for leaves to be seen from the adaxial side by a vehicle-mounted sensor in the field. In  
64 addition, the adaxial side of the leaf displayed the same type of kinetics of VBF changes upon  
65 infection<sup>5,7</sup>. This was the first demonstration of presymptomatic disease detection with real-  
66 time capacity for in field proximal sensing. None of the cited studies were done on naturally  
67 occurring infections.

68           The objective of this work was to follow naturally occurring infections from the local  
69 inoculum without knowing the time of infection. It was done on marked leaves in the field at  
70 various leaf levels in order to compare the Mx-330 sensing to visual assessments of the  
71 disease symptoms.

## 72   **Material and Methods**

### 73   **Experiment design**

74   Experiments were performed in an experimental vineyard near Blanquefort (Lat. 44.917° N,  
75 Long. 0.642° W) in the Bordeaux region (France) in 2014 on a north-south oriented row of  
76 *Vitis vinifera* cultivar Merlot Noir. Ten consecutive vine stocks were chosen and twelve  
77 leaves per stock were marked on May 23<sup>rd</sup> (BBCH 57, flowers separating), with six leaves per  
78 row side, both east and west. Leaves were selected at three canopy heights: low, middle and  
79 high, two leaves per height. This protocol produced six categories of leaves with 20 leaves per  
80 category and 120 marked leaves in total. Measurements started on May 23<sup>rd</sup> (day of the year  
81 (DOY) 143) and lasted until July 11<sup>th</sup> (DOY 192), with an overall frequency of two  
82 measurements per week. In the rare cases where a marked leaf was lost (accidentally  
83 detached), which happened six times during the whole experiment, it was replaced by a one  
84 nearby at the same height. No plant protection treatment was ever applied to this plot during  
85 the 2014 season. The weather data recorded during the survey are presented in Fig. S1 (see  
86 ESI†).

### 87   **Visual disease assessment**

88   Visual assessments of downy mildew, powdery mildew and black rot symptoms were made  
89 for every marked leaf in parallel to the Mx-330 measurements. The visual assessments only  
90 took into account the 6-cm central leaf area, which was measured using the Mx-330. The leaf  
91 severity was visually estimated independently for each disease. It was defined as the  
92 proportion of the leaf area with symptoms compared to the total 6-cm central leaf area. We  
93 used twelve classes for this estimation: 0 (no symptom), 1% (isolated spot), 10%, 20%, 30%,  
94 40%, 50%, 60%, 70%, 80%, 90% and 100%. The visual assessments were made without leaf  
95 side considerations.

96           For each leaf category we calculated: the ‘visual incidence’ as the percentage of  
97 infected leaves; the ‘visual leaf severity’ as the mean severity of infected leaves; and the  
98 ‘visual plot severity’ as the mean severity of all leaves (healthy leaf severity being zero).  
99 Although the measurements were performed on a single row, in this work we use the term

100 ‘plot severity’ by convention<sup>8</sup>. It should also be recalled that numerically plot severity =  
101 incidence x leaf severity. Given the experiment design, the estimation of both disease  
102 incidence and disease severity had to be calculated on a leaf basis, not on shoot or plant basis  
103 as it is usually done<sup>9</sup>.

#### 104 **Multiplex proximal sensing**

105 We used the new Multiplex 330 (FORCE-A, Orsay, France) proximal sensor<sup>5</sup>. Mx-330 is a  
106 hand-held, multi-parametric fluorescence sensor based on LED excitation and filtered-  
107 photodiode detection that is designed to work in the field under daylight condition. It is based  
108 on the mechanical structure and electronics of the Multiplex 3<sup>10</sup>, but specifically adapted to  
109 measure *in vivo* the stilbenoid VBF on grapevine leaves (335 nm excitation – 400 nm  
110 emission). The sensor illuminates a 6-cm-diameter area at a 4-cm distance from the sources  
111 and detectors. All marked leaves had a diameter exceeding 6 cm. The leaves were flattened as  
112 much as possible during the measurements by pressing them against the sensors with a hand  
113 covered by a black low-fluorescing glove. The Mx-330 measurements were performed on  
114 both leaf sides, the upper (adaxial) and the lower (abaxial). A UV-excited chlorophyll  
115 fluorescence (FRF\_UV) of the leaf could be measured simultaneously with VBF thanks to the  
116 presence of an additional far-red (750 nm) detector in the Mx-330.

#### 117 **Measurement filtering and index calculations**

118 We used the FRF\_UV signal to remove abnormal VBF measurements by looking at complete  
119 individual leaf kinetics. Indeed, a non-destructive measurement on the same leaf allowed us to  
120 easily identify an abnormal measurement in a temporal series. The FRF\_UV signal is  
121 independent of VBF fluorescence. It was rather constant during the whole survey (data not  
122 shown). However the FRF\_UV signal was sensitive to the operators’ diligence. A  
123 measurement triggered before the leaf was totally pressed against the sensor, a movement of  
124 the leaf during the measurement, direct strong sunlight entering the photodiode detector or an  
125 unknown effect can all produce an abnormal signal value. For each DOY and each leaf side,  
126 measurements with a FRF\_UV value larger than two standard deviations from the mean were  
127 removed, because this signal was not influenced significantly by the presence or absence of  
128 the disease. This procedure was repeated once. In the end, for the whole survey only 8.7% of  
129 the measurements were discarded by this procedure.

130 The 120 marked leaves were organised into six leaf categories: low, middle and high  
131 canopy heights at the east and the west sides of the row. For each category and each  
132 measurement day, two indices were calculated based on the Mx-330 measurements of VBF.

133 First, the 'VBF incidence' defined as the number of leaves having a VBF above a fixed  
134 threshold divided by the total number of leaves. To choose the threshold for each leaf side, we  
135 calculated the mean and standard deviation of all VBF measurements of DOY 143, 146 and  
136 148. Downy mildew symptoms were not observed on these dates. The threshold was defined  
137 as 2.7 standard deviations above the mean VBF. This value corresponds to the upper limit of  
138 a box plot and is close to the 99<sup>th</sup> percentile. With such a high threshold we were confident in  
139 selecting only infected leaves, i.e. to avoid false positives. Second, the 'VBF severity' index  
140 was calculated as the mean VBF value of all leaves of a given category.

141 Data were processed with the numerical/graphical software Igor 6 (WaveMetrics, Lake  
142 Oswego, Oregon).

## 143 **Results and discussion**

144 There was no powdery mildew infection during this particular survey. Black rot symptoms  
145 stayed low with a visual incidence below 15% and a maximum individual-leaf visual severity  
146 of 5%. The VBF signal of the leaves showing black rot symptoms without other disease  
147 symptoms was compared to the VBF signal of leaves showing no symptoms at all. No  
148 differences could be found (Fig. S2 in the ESI†). In addition, it is not known whether black  
149 rot induces synthesis and accumulation of stilbenoids in grapevine leaves. Therefore, the  
150 presence of black rot was not taken into account for a further analysis of the VBF of leaves.  
151 On the other hand, the downy mildew infection led to a severe epidemic. For these reasons we  
152 considered *P. viticola* as the main cause of the changes in VBF.

153 The grapevine leaf VBF measured with the Mx-330 can be the result of additive  
154 contributions of several fluorophores. In healthy leaves it is mainly due to hydroxycinnamic  
155 acids<sup>11</sup>. In *P. viticola* infected leaves the VBF of induced stilbenoids adds up to this  
156 autofluorescence<sup>3, 4</sup>. Moreover, the VBF of both healthy and infected grapevine leaves is  
157 always larger on the abaxial leaf side than on the adaxial one. This is why adaxial and abaxial  
158 VBF measurements need to be considered separately. Individual-leaf kinetics of VBF (Fig. 1)  
159 corresponded to the ones seen with artificial *P. viticola* infections in the greenhouse<sup>5</sup> and in  
160 the field<sup>7</sup>. Since the infections here occurred randomly from inoculum sources within the  
161 vineyard the date of appearance was different among leaves (Fig. 1). At the beginning of the  
162 measurement period, VBF levels measured by Mx-330 were around 60 mV and 95 mV, for  
163 the adaxial and the abaxial leaf sides, respectively, i.e. the usual level found in healthy leaves.  
164 It was followed by a significant transient increase in VBF with a highly variable VBF peak  
165 value. The VBF decreased thereafter with a general tendency to remain higher than in healthy

166 leaves. The VBF signal is also dependent on the percentage diseased area of the measured leaf  
167 surface. Therefore, the epidemic development of the polycyclic pathogen complicates the  
168 kinetics of the VBF signal because a variable portion of the leaf surface area can be infected  
169 by a primary and a secondary infection on the same leaf (Fig. 1, leaf n°1). Thus a global  
170 analysis of the VBF of a population of leaves was necessary to characterize the downy  
171 mildew infection at the plot level. For this global analysis we kept the six leaf categories  
172 separate: low, middle and high canopy heights at the east and the west row sides.

173 The VBF incidence kinetics for the six leaf categories were plotted separately for the  
174 adaxial (Fig. 2A) and the abaxial (Fig. 2B) leaf side and compared to visual incidence  
175 measurements (Fig. 2C). Each category is represented by the mean of 20 marked leaves. The  
176 VBF incidence was earlier than visual incidence. At DOY 168, depending on the leaf  
177 category, 15 to 45% of leaves were classified as infected by abaxial VBF incidence compared  
178 to only 0 to 10% by visual assessment. This was also true for adaxial VBF incidence but with  
179 a lower value, 5-10%, and only for two categories. Visual incidence was already 5% for two  
180 categories since DOY 157, but it should be noted that this 5% corresponded to a single leaf.

181 VBF incidence showed a clear valley at DOY 174-176 before a subsequent large  
182 increase and at a time when visual incidence was sharply increasing (Fig. 2A,B). This was the  
183 direct consequence of the bell-shaped kinetic of VBF following *P. viticola* infection<sup>5,7</sup> briefly  
184 described above (Fig. 1). When the VBF of the first infected leaves decreased after DOY 171  
185 it decreased under the threshold, so these leaves were not counted as infected anymore while  
186 the leaves infected in the second phase had a VBF still below the threshold (Fig. 1). The large  
187 increase in VBF incidence was slowing down after DOY 182, and was even decreasing for  
188 two categories on the adaxial side. This multi-phase behaviour, which was also seen using  
189 visual incidence, especially with the plateau at DOY 171-182, was most probably related to  
190 the succession of primary, secondary and even higher-order infections.

191 The three leaf categories (low, middle and high) were well separated during the last  
192 infection phase (DOY 182-192) both in the visual incidence (Fig. 2C) and in the adaxial VBF  
193 incidence (Fig. 2A). The difference in kinetics of the three categories of leaves can be linked  
194 to the epidemiology of downy mildew<sup>2</sup>. The primary inoculum is mainly found on the ground,  
195 closer to the low leaves contaminated by rain splashing<sup>12</sup>.

196 The effect of row side on leaf attributes<sup>13</sup>, especially photosynthesis<sup>14</sup>, is known for  
197 north/south oriented rows<sup>15,16</sup>, but it seems to be too subtle to reflect on downy mildew  
198 incidence (Fig. 2) The east/west row-side dichotomy had no significant influence on  
199 incidence nor severity, independent of the assessment technique.

200 Fig. 3 confirms that VBF may be used to estimate disease severity. As expected, the  
201 correspondence was better when abaxial VBF severity was compared to visual severity. In  
202 fact, the adaxial VBF showed significant severity only after DOY 180. Abaxial VBF severity  
203 (Fig. 3A) followed the visual leaf severity kinetics (Fig. 3B) and even more the visual plot  
204 severity kinetics (Fig. 3C). This implies that the proportion of infected leaf area containing  
205 stilbenoids influenced the VBF signal more than the stilbenoid content per unit surface area.

206 Visual leaf severity showed a transitory peak at DOY 168 for the east-low and west-  
207 high leaf categories. The decrease after the peak is a consequence of the appearance of newly  
208 infected leaves with lower severity after DOY 168. These newly infected leaves contribute  
209 mathematically to the decrease in the mean. This coincided with the appearance of the first  
210 visually detected infected leaves in three other categories (Fig. 2C and Fig. 3C). This is  
211 another sign of the beginning of the second phase of infection.

### 212 **Proximal sensing of diseases**

213 The temporal and spatial dynamics of plant pathogens can be quantified by visually assessing  
214 disease intensity (incidence and severity). However, the accuracy and precision of visual  
215 disease assessments performed by different raters continues to be called into question<sup>8</sup>. In  
216 addition, a sensitive automatic mapping of diseases is needed for precision pest  
217 management<sup>17</sup>. Indeed, until now the successful reflectance-based remote sensing of diseases  
218 was limited to the changes in green biomass due to defoliation<sup>8, 18</sup>. Fluorescence, although  
219 technically more demanding than reflectance, is a far more sensitive technique. Under  
220 practical agronomical conditions the difference is about a thousand fold. The theoretical  
221 sensing limit of fluorescence is a single molecule<sup>19</sup>. Furthermore, fluorescence can reveal  
222 molecules that absorb UV light, like stilbenoids, that cannot be seen by reflectance. Previous  
223 attempts to use fluorescence sensing in the field concerned yellow rust in wheat using a xenon  
224 lamp-based imaging spectrograph<sup>20, 21</sup>. More often, the experiments were restricted to  
225 greenhouses using, for example, laser-induced detection of chlorosis in citrus<sup>22</sup> or to the  
226 laboratory even when a UV lidar was used for wheat rust detection<sup>23</sup>. As reviewed recently<sup>17,</sup>  
227 <sup>24, 25</sup>, crop disease sensing using fluorescence in the field is still in its infancy. The latest  
228 attempt investigated leaf diseases in barley using the Multiplex 3 fluorescence sensor<sup>26</sup>.  
229 Thermal imagery is another interesting optical sensing technique<sup>27, 28</sup>. It was applied to downy  
230 mildew detection on grapevine, but only with artificial inoculation on individual leaves in the  
231 greenhouse<sup>28</sup>. This restriction was also applied in the latest attempt to use variable chlorophyll  
232 fluorescence imaging on *P. viticola* infected leaves<sup>29</sup>.



233 The present version of the sensor has a limited functioning distance to a few  
234 centimetres. This limits tractor-mounted sensing. However, an earlier version of the Multiplex  
235 was already mounted on a parallelogram frame (a ski) on a tractor in order to glide along the  
236 canopy and to allow continuous mapping of leaf characteristics<sup>30</sup>. With the development of  
237 new more powerful LEDs, UV-based non-contact fluorosensing from a larger distance will be  
238 possible. This was already done with the Multiplex 3.6<sup>31, 32</sup>. We are currently working on the  
239 implementation of such a powerful UV source to a new version of the sensor meant to be  
240 mounted on tractors for continuous mapping.

241 The variability of diseases in the field can be temporal, due to the kinetics of the  
242 infection, and spatial, because of the spreading of the infection from the initial hot spots.  
243 Therefore, both temporal and spatial surveys of diseases are important for efficient prevention  
244 and treatment. Even if not specific for the downy mildew<sup>33</sup>, the VBF has the advantage of  
245 detecting leaves with visible symptoms and can also detect asymptomatic early stage  
246 infections, even in the field, as shown in this work. The advantages of early and automatic  
247 detection of disease outbreaks will be twofold. First, it would help viticulturists to choose the  
248 right curative plant protection product, a group known to be more efficient in the early phases  
249 of infection<sup>1</sup>. Second, it would provide objective information on the first primary infection  
250 that is needed as an input variable for forecast models based on meteorological data<sup>2, 34, 35</sup>.  
251 The VBF-based method will allow an early detection of suspicious hot spots or larger zones  
252 of the vineyard. The subsequent identification of the origin of the disease or of the abiotic  
253 stress can be done by other more specific sampling techniques. The automatic mapping will  
254 also be useful in order to comply with the European regulation for organic viticulture. This  
255 regulation (EC 834/2007) allows the application of authorised plant protection products only  
256 in case of an established threat to the crop. Mounted fluorescence sensors on tractors will  
257 allow these surveys while the grower is performing other viticultural practices: hedging,  
258 leafing, fertilisation or spraying. This time-sharing approach would be the most economic,  
259 without precluding specific survey services.

## 260 **Conclusion & Prospects**

261 We showed that stilbenoid VBF is a valuable signal to detect and monitor naturally occurring  
262 downy mildew epidemic in vineyards. At the same time, we also showed that the Mx-330 is  
263 an adequate tool for this measurement on a leaf-to-leaf basis. The presence of this signal on  
264 the adaxial side of leaves makes it suitable for vehicle-mounted proximal sensing. Based on  
265 the Mx-330 VBF measurements we proposed two indices 'VBF incidence' and 'VBF

266 severity'. They were both linked to the downy mildew disease intensity when this disease was  
267 the only one present. They are comparable to the information given by visually assessed  
268 disease incidence and severity. This should be confirmed and refined on a larger scale and  
269 using repeated experiments. This approach should also be tested for the detection of powdery  
270 mildew, which was not present in the experimental plot in 2014.

271 This new approach using phytoalexin-based fluorescence can be generalised to other  
272 crops like resveratrol fluorescence in peanuts or coumarin fluorescence in sunflower, for  
273 example. We need to detect the disease in the field in order to achieve the goal of precision  
274 agriculture: put the right doses, to the right place, at the right time. This will decrease the  
275 pollution of the environment by pesticide treatments. It will also help to protect the grape  
276 growers and the produced wine from contamination.

### 277 **Acknowledgements**

278 This work received funding from the European Community's Seventh Framework  
279 Program (FP7/2007-2013) under Grant Agreement FP7-311775, Project Innovine. This work  
280 was supported by FORCE-A (Orsay) in a joint project with Centre National de la Recherche  
281 Scientifique and Université Paris-Sud (grant UPS N8780). The authors would like to thank  
282 Dr. Zorana Ratkovic for the proofreading of the manuscript and the anonymous reviewers for  
283 comments that helped to improve the clarity of the paper.

284

### 285 **Notes and References**

286 The article is a contribution to the 16th ICP Cordoba Congress publications.

- 287 1. R. Muthmann, *The use of plant protection products in the European Union - Data*  
288 *1992-2003*, Office for Official Publications of the European Communities - Eurostat,  
289 Luxembourg, 2007.
- 290 2. C. Gessler, I. Pertot and M. Perazzolli, *Plasmopara viticola*: a review of knowledge  
291 on downy mildew of grapevine and effective disease management, *Phytopathol.*  
292 *Mediterr.*, 2011, **50**, 3-44.
- 293 3. A. Poutaraud, G. Latouche, S. Martins, S. Meyer, D. Merdinoglu and Z. G. Cerovic,  
294 Fast and local assessment of stilbene content in grapevine leaf by *in vivo* fluorometry,  
295 *J. Agric. Food Chem.*, 2007, **55**, 4913 - 4920.

- 296 4. S. Bellow, G. Latouche, S. C. Brown, A. Poutaraud and Z. G. Cerovic, *In vivo*  
297 localization at the cellular level of stilbene fluorescence induced by *Plasmopara*  
298 *viticola* in grapevine leaves, *J. Exp. Bot.*, 2012, **63**, 3697-3707.
- 299 5. S. Bellow, G. Latouche, S. C. Brown, A. Poutaraud and Z. G. Cerovic, Optical  
300 detection of downy mildew in grapevine leaves: daily kinetics of autofluorescence  
301 upon infection, *J. Exp. Bot.*, 2013, **64**, 333-341.
- 302 6. G. Latouche, S. Bellow, A. Poutaraud, S. Meyer and Z. G. Cerovic, Influence of  
303 constitutive phenolic compounds on the response of grapevine (*Vitis vinifera* L.)  
304 leaves to infection by *Plasmopara viticola*, *Planta*, 2013, **237**, 351-361 .
- 305 7. G. Latouche, A. Poutaraud, S. Bellow, S. Evain, L. Ley, S. C. Brown and Z. G.  
306 Cerovic, Detection of downy mildew in the field on grapevine leaves using a new  
307 portable fluorescence sensor, in 7th International Workshop on Grapevine Downy and  
308 Powdery Mildew, 2014, pp. 118-121.
- 309 8. F. W. J. Nutter, N. van Rij, S. K. Eggenberger and N. Holah, in *Precision Crop*  
310 *Protection - the Challenge and Use of Heterogeneity*, eds. E.-C. Oerke, R. Gerhards,  
311 G. Menz and R. A. Sikora, Springer, Dordrecht Heidelberg London New York, 2010,  
312 pp. 27-50.
- 313 9. A. Calonnec, P. Cartolaro and J. Chadoeuf, Highlighting features of spatiotemporal  
314 spread of powdery mildew epidemics in the vineyard using statistical modeling on  
315 field experimental data, *Phytopathology*, 2009, **99**, 411-422.
- 316 10. N. Ben Ghazlen, Z. G. Cerovic, C. Germain, S. Toutain and G. Latouche, Non-  
317 destructive optical monitoring of grape maturation by proximal sensing, *Sensors*,  
318 2010, **10**, 10040-10068.
- 319 11. Z. G. Cerovic, G. Samson, F. Morales, N. Tremblay and I. Moya, Ultraviolet-induced  
320 fluorescence for plant monitoring: present state and prospects, *Agronomie: Agric.*  
321 *Environ.*, 1999, **19**, 543-578.
- 322 12. V. Rossi and T. Caffi, The role of rain in dispersal of the primary inoculum of  
323 *Plasmopara viticola*, *Phytopathology*, 2012, **102**, 158-165.
- 324 13. R. S. Jackson, *Wine Science - Principles and Applications*, Elsevier (Academic Press),  
325 2008.
- 326 14. H. R. Schultz, Extension of a Farquhar model for limitations of leaf photosynthesis  
327 induced by light environment, phenology and leaf age in grapevines (*Vitis vinifera* L.  
328 cvv. White Riesling and Zinfandel), *Funct. Plant Biol.*, 2003, **30**, 673-687.

- 329 15. J. E. Jackson and J. W. Palmer, Interception of light by model hedgerow orchards in  
330 relation to latitude, time of the year and hedgerow configuration and orientation, *J.*  
331 *Appl. Ecol.*, 1972, **9**, 341–358.
- 332 16. S. E. Spayd, J. M. Tarara, D. L. Mee and J. C. Ferguson, Separation of sunlight and  
333 temperature effects on the composition of *Vitis vinifera* cv. Merlot berries, *Am. J.*  
334 *Enol. Vitic.*, 2002, **53**, 171-182.
- 335 17. A.-K. Mahlein, E.-C. Oerke, U. Steiner and H.-W. Dehne, Recent advances in sensing  
336 plant diseases for precision crop protection, *Eur. J. Plant Pathol.*, 2012, **133**, 197-209.
- 337 18. F. Mazzetto, A. Calcante, A. Mena and A. Vercesi, Integration of optical and analogue  
338 sensors for monitoring canopy health and vigour in precision viticulture, *Precis.*  
339 *Agric.*, 2010, **11**, 636-649.
- 340 19. B. Valeur, *Molecular Fluorescence. Principles and Applications*, Wiley-VCH,  
341 Weinheim - New York - Chichester - Brisbane -Singapore - Toronto, 2002.
- 342 20. L. Bodria, M. Fiala, R. Oberti and E. Naldi, Chlorophyll fluorescence sensing for  
343 early detection of crop's diseases symptoms, in ASAE Annual International Meeting,  
344 ASAE, 2002, pp. 1-10.
- 345 21. C. Bravo, D. Moshou, R. Oberti, J. S. West, A. McCartney, L. Bodria and H. Ramon,  
346 Detection of foliar disease in the field by the fusion of measurements made by optical  
347 sensors, in ASAE Annual International Meeting / CIGR XVth World Congress,  
348 ASAE, 2002, pp. 1-12.
- 349 22. J. J. Belasque, M. C. G. Gasparoto and L. G. Marcassa, Detection of mechanical and  
350 disease stresses in citrus plants by fluorescence spectroscopy, *Appl. Optics*, 2008, **47**,  
351 1922-1926.
- 352 23. W. Lüdeker, H.-G. Dahn and K. P. Günther, Detection of fungal infection of plants by  
353 laser-induced fluorescence: An attempt to use remote sensing, *J. Plant Physiol.*, 1996,  
354 **148**, 579-585.
- 355 24. F. Hahn, Actual pathogen detection: sensors and algorithms - a review, *Algorithms*,  
356 2009, **2**, 301-338.
- 357 25. S. Sankaran, A. Mishra, R. Ehsani and C. Davis, A review of advanced techniques for  
358 detecting plant diseases, *Comput. Electron. Agric.*, 2010, **72**, 1-13.
- 359 26. K. Yu, G. Leufen, M. Hunsche, G. Noga, X. Chen and G. Bareth, Investigation of leaf  
360 diseases and estimation of chlorophyll concentration in seven barley varieties using  
361 fluorescence and hyperspectral indices, *Rem. Sens.*, 2014, **6**, 64-86.

- 362 27. H.-E. Nilsson, Remote sensing and image analysis in plant pathology, *Annu. Rev.*  
363 *Phytopathol.*, 1995, **15**, 489-527.
- 364 28. M. Stoll, H. R. Schultz, G. Baecker and B. Berkelmann-Loehnertz, Early pathogen  
365 detection under different water status and the assessment of spray application in  
366 vineyards through the use of thermal imagery, *Precis. Agric.*, 2008, **9**, 407-417.
- 367 29. L. Csefalvay, G. Di Gaspero, K. Matous, D. Bellin, B. Ruperti and J. Olejnickova,  
368 Pre-symptomatic detection of *Plasmopara viticola* infection in grapevine leaves using  
369 chlorophyll fluorescence imaging *Eur. J. Plant Pathol.*, 2009, **125**, 291-302.
- 370 30. S. Debuisson, C. Germain, O. Garcia, L. Panigai, D. Moncomble, M. Le Moigne, E.  
371 M. Fadaïli, S. Evain and Z. G. Cerovic, Using Multiplex<sup>®</sup> and greenseeker<sup>™</sup> to  
372 manage spatial variation of vine vigor in Champagne, in 10th ICPA, 2010, pp. 1-21.
- 373 31. L. Longchamps and R. Khosla, Early detection of nitrogen variability in maize using  
374 fluorescence, *Agron. J.*, 2014, **106**, 511.
- 375 32. N. Tremblay, Sensing technologies in horticulture: options and challenges, *Chron.*  
376 *Hort.*, 2013, **53**, 10-14.
- 377 33. J. Chong, A. Poutaraud and P. Huguency, Metabolism and roles of stilbenes in plants,  
378 *Plant Science*, 2009, **177**, 143-155.
- 379 34. V. Rossi, F. Salinari, S. Poni, T. Caffi and T. Bettati, Addressing the implementation  
380 problem in agricultural decision support systems: the example of vite.net<sup>®</sup>, *Comput.*  
381 *Electron. Agric.*, 2014, **100**, 88-99.
- 382 35. M. Raynal, C. Debord, S. Guittard and M. Vergnes, Epicure, a geographic information  
383 decision support system applied on downy and powdery risks of mildews epidemics  
384 on the Bordeaux vineyard, in 6th International Workshop on Grapevine Downy and  
385 Powdery Mildew, INRA, 2010, pp. 144-146.

386  
387

## 388 **Figure captions**

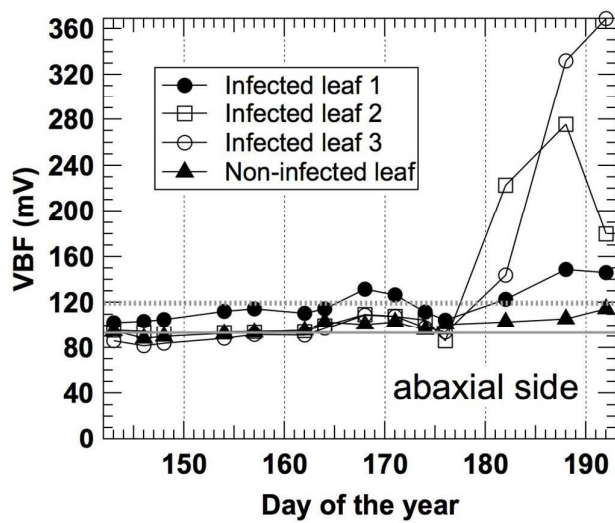
389 Figure 1. Examples of violet-blue fluorescence (VBF) kinetics of the abaxial side of three  
390 individual leaves naturally infected by downy mildew compared to a non-infected leaf. The  
391 non-infected leaf did not show any visual symptom until the end of the 50-days survey. The  
392 horizontal grey line and the grey dotted line are the mean VBF value for healthy leaves and  
393 the 2.7 standard deviations above the mean used as the threshold for incidence detection,  
394 respectively.

395

396 Figure 2. Adaxial (A) and abaxial (B) leaf sides violet-blue fluorescence (VBF) incidence  
397 compared to the visual incidence (C). Six categories of leaves with 20 marked leaves each  
398 were followed for 50 days during a naturally occurring downy mildew infection. Leaves were  
399 grouped in categories by their position in the canopy: low, middle and high, on the East or  
400 West side of a North/South oriented row.

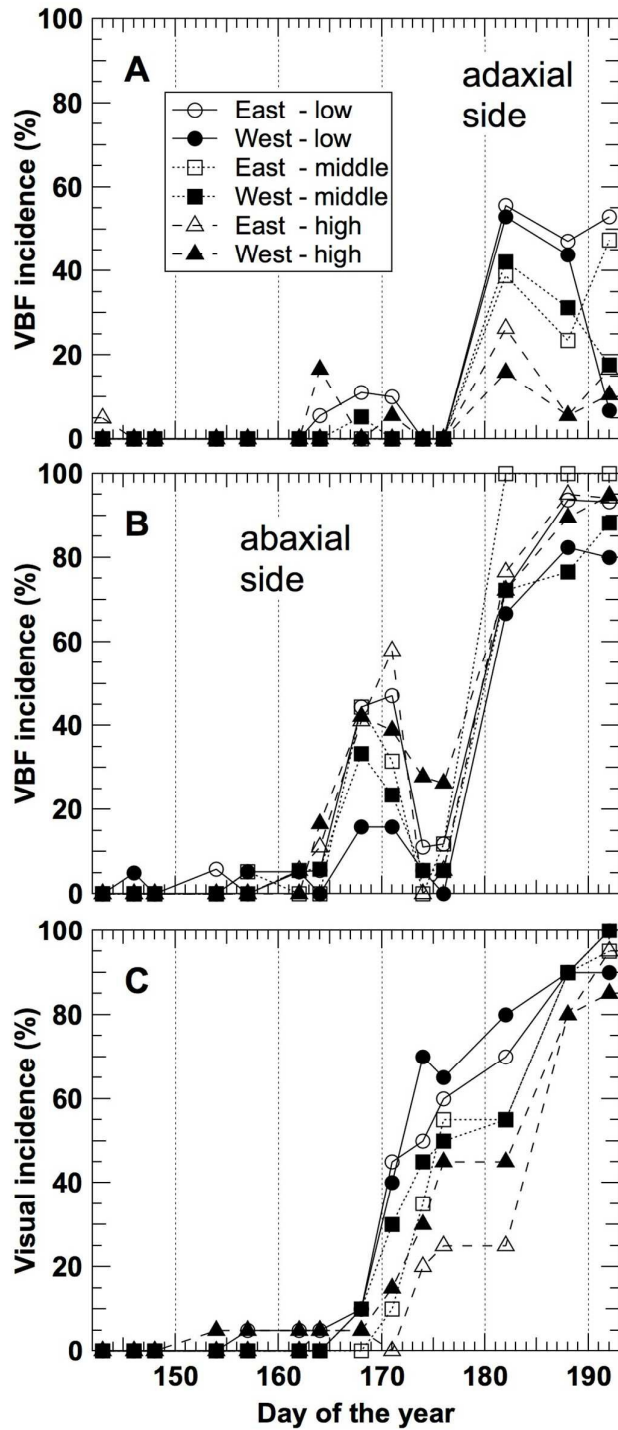
401

402 Figure 3. Adaxial and abaxial leaf side violet-blue fluorescence (VBF) severity (A) compared  
403 to the visual leaf severity (B) and visual plot severity (C). Six categories of leaves with 20  
404 marked leaves each were followed for 50 days. Leaves were grouped in categories by their  
405 position in the canopy: low, middle and high, on the East or West side of a North/South  
406 oriented row. The two horizontal grey lines are the mean of the abaxial and the adaxial leaf  
407 side VBF measurements obtained from all healthy leaves before the *P. viticola* infection  
408 (DOY 143, 146 and 148).

409 **FIGURES**

410

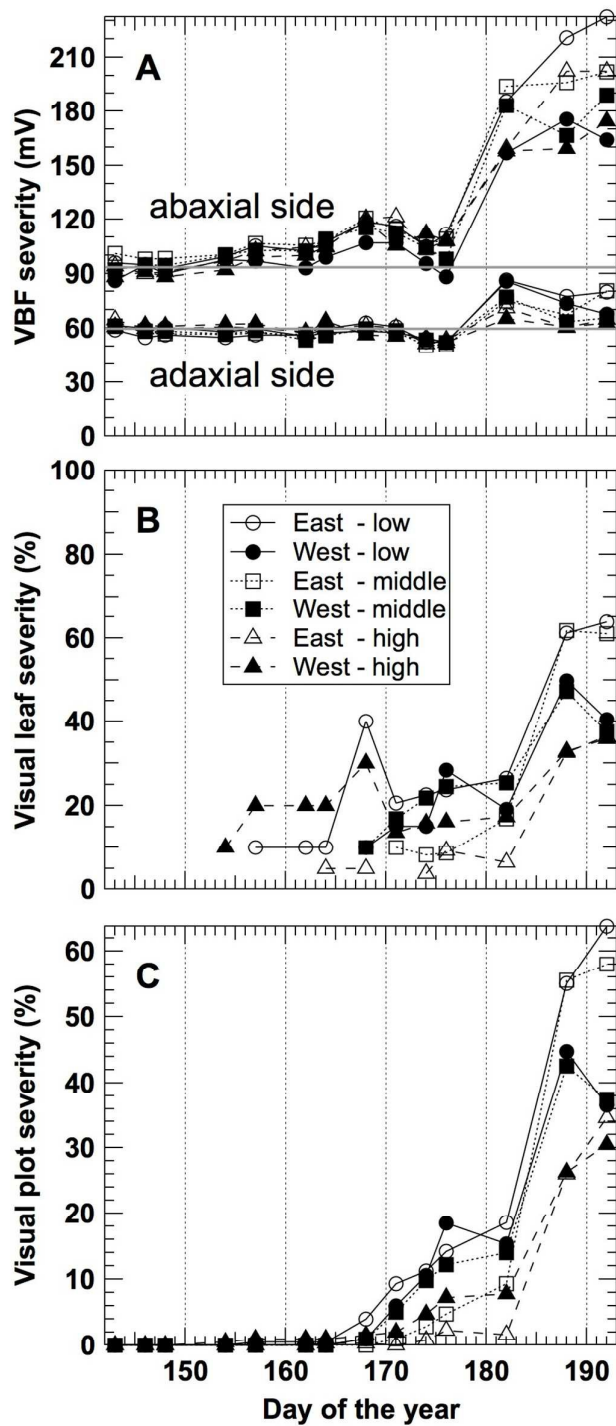
411 Figure 1.



412

413 Figure 2.





414

415 Figure 3.



The presence of a major grapevine disease was detected in the field by a new fluorescence proximal sensor. The approach based on UV-induced fluorescence of phytoalexins can be extended to vineyard mapping.

225x140mm (72 x 72 DPI)